Polarization Assisted Phase Sensitive Processor

F. Parmigiani, G. Hesketh, R. Slavík, P. Horak, P. Petropoulos, D. J. Richardson

Abstract— We propose and experimentally demonstrate a phase sensitive optical processor, capable of generating two co-directional and π–phase shifted phase sensitive amplifiers (PSAs) in a single device. Phase-sensitive operation is obtained by polarization mixing a phase-locked signal/idler pair generated in a degenerate dual-pump vector parametric amplifier based on four-wave mixing (FWM) in a highly nonlinear fiber (HNLF). We refer to this configuration as a polarization assisted PSA (PA-PSA) and demonstrate some of the applications that it may find. Firstly, we experimentally demonstrate the regeneration of a binary phase shift keying (BPSK) signal in a system that requires only a very low nonlinear phase shift (NPS) of 0.35 rad. Secondly, we decompose a quadrature phase shift keying (QPSK) signal into its in-phase and quadrature components. Whilst application to a QPSK signal is shown in our demonstration we demonstrate numerically that any complex modulation format signal can be decomposed using this approach. Finally, we use our processor to regenerate QPSK signals in a single non-linear device.

***Index Terms*—Four wave mixing, nonlinear optics, phase sensitive amplifiers.**

I. Introduction

Both phase insensitive and phase sensitive (PS) FWM schemes are often used as the basis for achieving optical processing of spectrally efficient modulation formats, which utilize both the phase and amplitude of the optical carrier. Some processing applications that have already been demonstrated include wavelength conversion [1-7], phase regeneration [8-13], electric field decomposition of phase shift keying (PSK) signals [14-16] and analogue-to-digital conversion (ADC) [17]. Single- and dual-pump configurations with the signal, idler and pump(s) being aligned either along the same polarization axis (scalar schemes) or on different polarization axes (vector schemes) and either non-degenerate or degenerate configurations (with the signal and idler being at either different or the same frequency, respectively) have been demonstrated [8-21]. In many of the applications above, for example, both PSA-based regeneration of BPSK signals and electric field decomposition of, in principle, any advanced modulation format require an ideal binary step-like phase response. This is usually achieved by generating a complex conjugate copy (idler) of the signal through PS-FWM, and coherently adding the two together. The relative strength of the two waves determines the phase sensitive extinction ratio, PSER (defined as the difference between the maximum PS gain and the maximum PS de-amplification), and in turn the steepness of the steps in the phase response. For an ideal step-like response, the two components should have identical power [8-9]. Indeed, to generate phase conjugated copies of similar signal strength a large non-linear interaction is needed, requiring for example, Watt-level pump powers in a HNLF.

It would be more energy- and cost- efficient, however, if large PSERs could be achieved at low pump powers. To this end, by carefully balancing the fiber parameters and the pump/signal powers and wavelengths, higher-order FWM components have been exploited in order to enhance the PS de-amplification term and hence to provide a large asymmetric PSER in a scalar configuration (achieved by obtaining a much larger PS deamplification than PS amplification). Using this scheme, BPSK regeneration and separate in-phase and quadrature decomposition were demonstrated in [11] and [14], respectively, at nonlinear phase shifts (NPSs) (defined as the product of the total pump power, the nonlinear coefficient and the fiber length) as low as 0.8 rad, providing a PSER of ~25 dB.

A more efficient way to optimize the coherent addition of the signal/idler pair (and achieve high PSERs) would be to perform this summation in a different physical dimension, for example at a different wavelength (to the signal) [15-16, 22], so that it would be possible to independently control and access their relative weights without the requirement of generating too much idler in the first place. It is worth pointing out though that such flexibility may come at the price of reduced net phase sensitive amplification and optical signal to noise ratio (OSNR) of the final signal. By exploiting this very concept, an asymmetric PSER of about 20 dB was achieved using hybrid optical phase squeezers to demonstrate the simultaneous phase regeneration of two coherent BPSK signals [22]. Alternatively, one may utilize the polarization dimension, e.g., we have recently demonstrated a PSA scheme that uses polarization mixing of a phase-locked signal-idler pair in a degenerate fiber optic parametric amplifier with two orthogonally polarised pumps and which we refer to as polarization-assisted PSA. Using this scheme an asymmetric PSER of ~26 dB (and thereby almost ideal binary step-like phase response) at NPSs as low as 0.3 rad was demonstrated [20]. Moreover, as the pumps in the PA-PSA are orthogonally polarized, the strength of the undesired FWM interaction between them is drastically reduced (a reduction of 30 dB relative to a scalar PSA was observed for a total launched power into the HNLF of 20 dBm), thereby substantially reducing the optical bandwidth occupied by the PA-PSA relative to the scalar case. This significantly improves the potential for scaling the process to a larger number of wavelength division multiplexed (WDM) channels, that could in principle be accommodated within the same spectral window. Following the preliminary results presented in [23-24], we herein evaluate the performance of this new technique to optically process coherent signals, demonstrating several examples. In more detail, the PA-PSA is first employed for the phase regeneration of a single BPSK signal at a NPS of

Dr F. Parmigiani gratefully acknowledges the support from the Royal Academy of Engineering/EPSRC through a University research Fellowship. This work was supported by the EPSRC grant EP/I01196X: Transforming the Future Internet: The Photonics Hyperhighway. The authors are with the Optoelectronics Research Centre, University of Southampton, Southampton SO17 1BJ, U.K. (e-mail: frp@orc.soton.ac.uk).

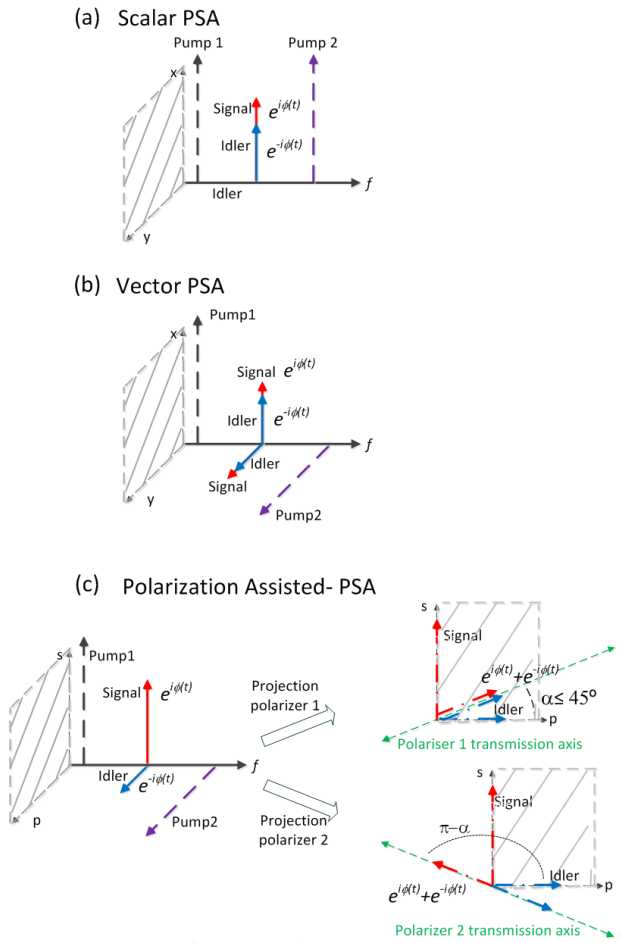

Fig.1: Schematic configurations of degenerate dual-pump (a) scalar, (b) vector and (c) polarization-assisted PSAs, respectively.

0.35 rad. Bit error ratio (BER) curves show a sensitivity improvement of about 2 dB relative to input signals that are affected by different levels of both single tone and broadband phase noise. In subsequent examples, we use another key feature of the proposed PA-PSA, which is its capability to obtain two co-directional and π-phase shifted PSAs in the same nonlinear medium, thus, dramatically improving the phase coherence of the various waves propagating in the PSAs if their recombination is desired.

The paper is organized as follows: in Section II, we describe the operating principle of the PA-PSA scheme. Section III discusses the experimental set-up used to demonstrate the new PA-PSA scheme. Section IV reports the experimental results of the all-optical phase regenerator of a single BPSK signal at low NPSs. Section V reports the experimental results of the electric field decomposition of the in-phase and quadrature components of a QPSK signal at different pump power levels. Regeneration of a QPSK signal is reported in Section VI. Finally, we draw our conclusions in Section VII.

II. Polarization Assisted PSA Operating Principle

Dual pump degenerate PSA configurations usually have either the input signal and pumps co-polarized with each other (scalar PSA), see Fig.1 (a), or the input signal is split evenly between the two polarizations of the orthogonally polarized pumps (vector PSA) [18]. Fig.1 (b) depicts the specific case of the signal linearly polarized at π/4 (half of the signal is co-polarized with one pump and the other half is co-polarized with the other) with respect to the two orthogonal, linearly polarized pumps. Each phase-locked complex conjugate copy (idler) generated in the nonlinear medium by one half of the signal interferes directly with the other half of the signal, producing PS amplification, since they share the same frequency and polarization [18]. Note, however, that a variety of PSERs can be achieved at a fixed pump power for any signal and idler polarization states, as long as they are not orthogonal to each other [25]. The generation of the idler and its coherent addition with the signal take place simultaneously in the nonlinear medium and can be described by the following signal transfer function:

$$A(t)e^{i\theta(t)} \propto e^{i\phi(t)}+me^{-i\phi(t)}, \quad (1)$$

where $A(t)$ and $\theta(t)$ are the output signal electric field amplitude and phase, respectively, $\phi(t)$ is the input signal phase, m is the weight of the idler in respect to the signal. (For the sake of clarity, the phases of the two pumps are set to zero and no pump depletion is considered.)

In the PA-PSA scheme, the signal and pumps are still phase-locked at the input of the system as in all PSA schemes, the pumps are orthogonally polarized as in the vector PSA, but the signal is co-polarized with only one of them, as shown in Fig.1 (c). In this instance, the idler is generated in a phase insensitive manner at the same frequency as the signal, but on the orthogonal polarization axis, therefore no interference (no PS operation) between signal and idler is achieved along any of the two polarization axes. However, if a polarizer is placed at the output of the nonlinear medium with its polarization angle properly rotated at an angle α (or π−α) with respect to the idler's axis (depending on the strength of the generated idler and, thus, on the pump power), then it is possible to exactly match the projected power of the signal and idler beams along the polarizer transmission axis. In other words, the polarizer allows the coherent addition of the projection of the signal and its phase-locked idler along its transmission axis as described in Eq. 1 and, thus, allows PS operation. Even in the instance when the generated idler is significantly weaker than the signal, i.e. at low pump powers, the signal/idler powers can be equalized via the angle α (π−α), guaranteeing an excellent phase squeezing response. It is worth noting, however, that at low NPSs, it is the PS de-amplification that is predominantly responsible for achieving high PSERs, and the PSA does not provide any net signal amplification.

Figure 2 shows two examples of the calculated amplitude and phase responses versus input signal phase, obtained from Eq. (1) for $m=0.3$ and $m=0.9$, achieving PSER values of about 5 dB and 26 dB, which are typical values achieved in the respective cases of the scalar and the PA-PSA implementations discussed in the rest of this manuscript at a total input power of 20 dBm. The figure highlights the relation between high PSERs (achieved by matching the signal and idler weights) and binary step-like phase responses.

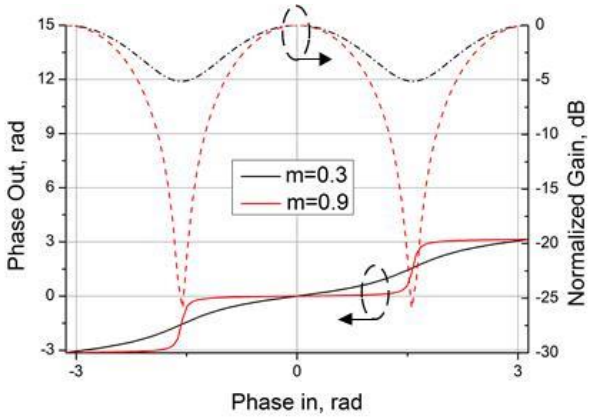

Fig.2: Typical (calculated) amplitude (dashed-dotted line) and phase (solid line) responses versus input signal phase for m=0.3 (black lines) and m=0.9 (red line).

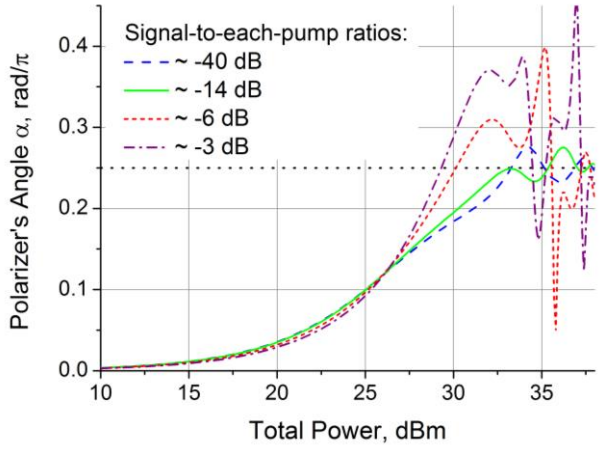

Fig.3: Numerical simulation of the polarizer angle, α, as a function of the total input power into the nonlinear media (HNLF in the specific case) for various input signal-to-pump ratios.

Fig. 3 shows the simulated optimum polarizer transmission angle, α, as a function of the total input power (the sum of signal and pump powers) for various power ratios of the signal to each of the pumps at the input of the HNLF (-40 dB (blue dashed line), -14 dB (green solid line), -6 dB (red short-dashed line) and -3 dB (purple dash-dot line)), while considering the two pump powers to be equal. Note that the same characteristics could be obtained by rotating the input signal polarization by π/2. The numerical results were obtained using the split-step approach to solve a set of two coupled generalized Nonlinear Schrödinger Equations (NLSEs) for the two orthogonal polarization components [26, 27] for pulse propagation through the HNLF, which was not assumed to be randomly birefringent along the fiber length as a first approximation [28]. As expected, at high powers, the generated idler and the signal have similar powers and the optimum angle becomes π/4 (or 3/4 π), implying that the PA-PSA power requirements resemble those of a conventional vector PSA. The oscillations in all the plots at high powers are due to the saturation of the parametric amplifier, periodically causing the generated idler power to become higher/smaller

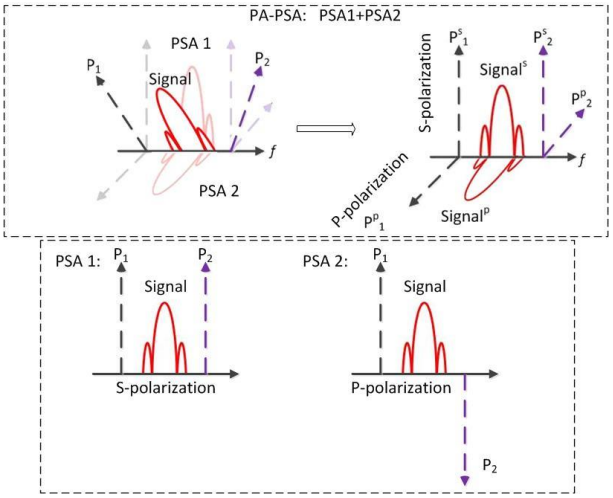

Fig.4: Synthesis example of the two π-phase shifted PSAs in a single medium, resulting in the PA-PSA scheme (when the idler is as strong as the signal, achieving two orthogonal PSAs).

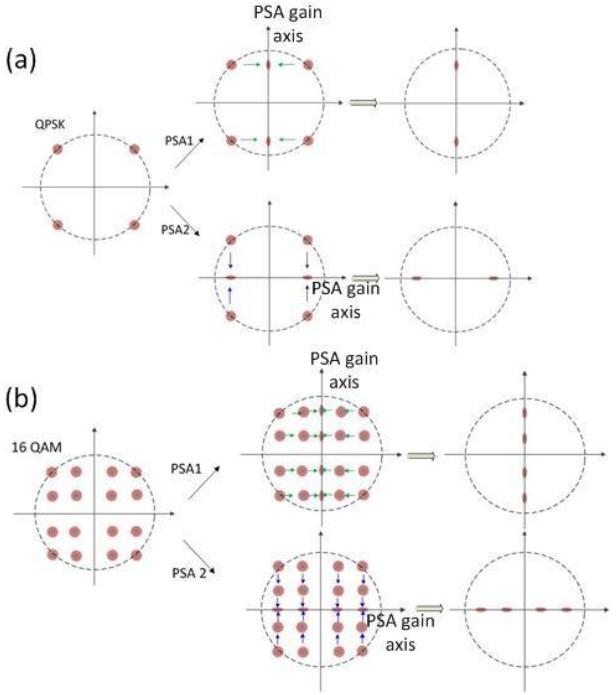

Fig.5: Schematics of two examples of optical field quadrature decomposition for QPSK (a) or 16 QAM (b).

than that of the signal and, thus, causing the polarizer's angle to be tuned closer to/further away from the signal axis to achieve optimum PS operation. Intuitively, as the signal power approaches the pump power at the input of the HNLF, such ringing becomes more significant and the minimum total power to reach α=π/4 decreases. On the other hand, at low powers the polarizer's transmission axis is very close to the polarization axis of the idler. For example, for a total power of 20 dBm (similar to the one used in the experiment described in Sections III and IV), α is about π/30, implying that the output signal will be attenuated by almost 10 dB after passing through the polarizer.

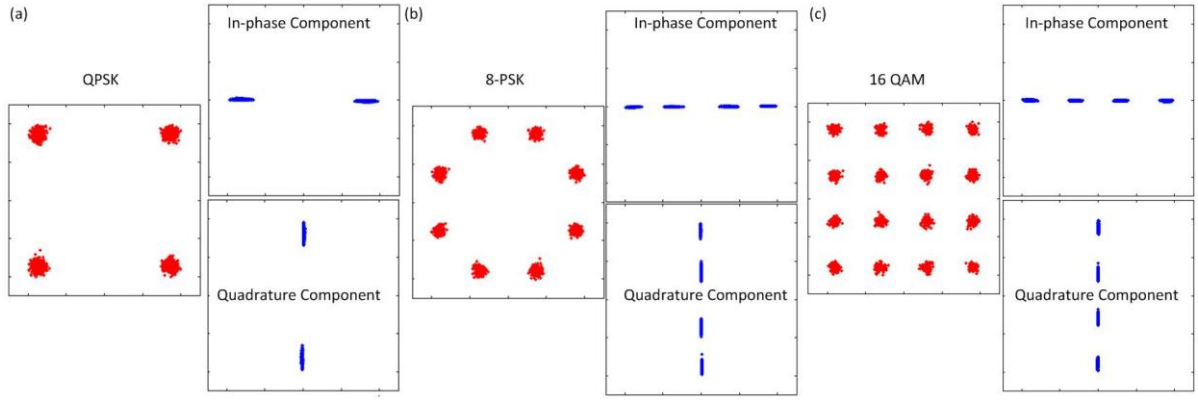

Fig.6: Simulated constellation diagrams at the input/output of the PA-PSA for QPSK (a), 8-PSK (b) and 16 QAM (c).

It is worth noting that in Fig.1 (c) the two possible polarization angles of the PA-PSA (α or $\pi-\alpha$) result in vector summations between the signal and idler that are π-phase shifted relative to each other. This effect can be exploited to give rise to the decomposition of the electric field of a signal to its two quadratures, and Fig. 4 attempts to explain this procedure. Assuming for simplicity the high power case presented above ($\alpha=\pi/4$), a geometrical analysis of the PA-PSA to two orthogonal systems (as in the top row of Fig. 4) reveals that it is constituted of two scalar PSAs that are π-phase shifted relative to each other (bottom row of Fig. 4). From Fig. 4 (top-right) it can be appreciated that aligning the transmission axis of a polarizer to either of the two PSAs (at $\pm\pi/4$ relative to the input signal polarization), it is possible to extract each PSA's output, i.e. the projection of each one quadrature. Then a polarization beam splitter (PBS) in place of the polarizer will simultaneously extract the two PSA outputs and decompose the incoming signal into its quadrature components. Figure 5 shows a schematic of how a binary-step PSA can decompose a signal into its real and imaginary parts, for the specific cases of QPSK and 16-quadrature amplitude modulation (16-QAM) signals. Figure 6 shows the corresponding numerical results for QPSK, 8-PSK and 16 QAM signals using the PA-PSA. These results were achieved for a NPS of 0.35 rad, implying that two independent polarizers rotated by α and $\pi-\alpha$, respectively, need to be used. However, similar results could be achieved for higher NPS values, where α approaches $\pi/4$, and in this case a single PBS can be used. Furthermore, it is worth noting that, for the specific case of QPSK as the incoming signal, each of the two PSA outputs represents an individually regenerated BPSK stream. Zheng et al. proposed and numerically investigated a scheme in [29], in which a pair of two independent PSAs (π-phase shifted relative to each other) was used in order to suppress the phase and amplitude noise fluctuations of QPSK signals. This scheme required recombination of the outputs of the two PSAs, which would be extremely difficult to implement in practice, due to phase coherence issues. However, by using a PA-PSA (in one fiber) any multi-path length fluctuation related issues are mitigated and coherence is preserved with significant practical implications. Figure 7 shows simulated constellation diagrams before and after the PA-PSA, where the polarizer is aligned to the signal (idler)

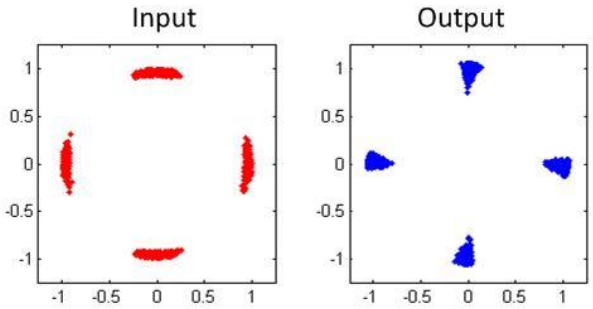

Fig.7: Simulated constellation diagrams for noisy incoming QPSK signals at the input/output of the PA-PSA operating for a total input power of 30 dBm.

axis. The PA-PSA operates at a total input power of 30 dBm and the signal-to-each-pump ratio is maintained at around -2 dB. Note that the generated higher-order FWM components play a key role in the proposed QPSK regeneration scheme. In particular, to achieve a QPSK transfer function, to a first approximation, the conjugated 3rd order phase harmonic needs to coherently add with the signal [10, 29]. An equivalent discussion could be carried out for a polarizer aligned to the idler polarization. The incoming QPSK signal is affected with Gaussian amplitude and phase root mean square (rms) noise of 1.4 % and 0.1 rad, respectively, and the final signal has an amplitude and phase rms of 5.2 % and 0.03 rad, respectively, achieving a phase squeezing factor of three, albeit with an increase of amplitude noise.

III. Experimental Set-up

Figure 8 shows the experimental set-up of the dual pump degenerate PA-PSA we implemented. An overdriven amplitude modulator (AM) was used to generate an optical frequency comb with ~50 GHz line spacing from a 17 dBm, 1557.4 nm continuous wave (CW) laser. A typically obtained spectrum is shown in Fig. 8 (left inset). The comb was filtered and demultiplexed using a programmable filter (Finisar Waveshaper – WS) to separately select three lines of the comb to act as the phase-locked signal and pump waves, respectively. This implementation was chosen for convenience; for real-system applications, a pump-signal synchronization scheme would need to be employed instead and its feasibility has been demonstrated in [9- 10]. The two

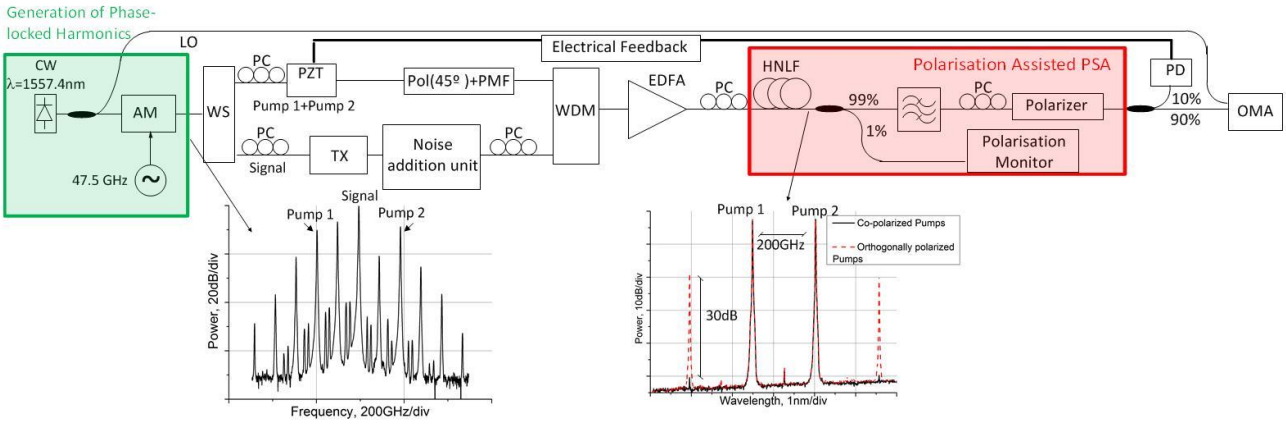

Fig.8: Experimental set-up of the polarization-assisted PSA scheme at low NPS. Inset figures: Initial optical comb spectrum and optical spectrum at the HNLF output when only the pumps were co- polarized (red dashed line) or cross-polarized (black solid line) for a total input power of about 20dBm (OSA resolution of 0.01nm). AM: amplitude modulator, PM: phase modulator, TX: transmitter, WDM: wavelength division multiplexer, PC: polarization controller; OSA: optical spectrum analyser, EDFA: erbium-doped fiber amplifier.

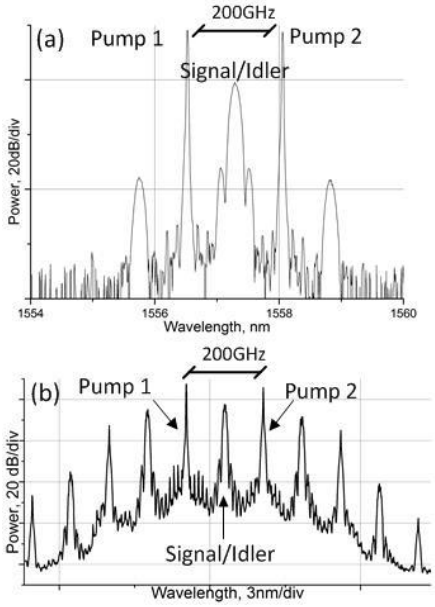

Fig.9: Example of optical spectral traces at the HNLF output for a total power at the input of the HNLF of about 20dBm (a) and 30 dBm (b), respectively (OSA resolution of 0.01nm).

pumps (Pump 1 and Pump 2), spaced by ~200 GHz, were linearly polarized and aligned at $\pi/4$ with respect to the primary polarization axis of a carefully chosen short length (about 2 m) of polarization maintaining fiber (PMF) to ensure their orthogonality at the HNLF input [21]. An example of the optical spectrum at the output of the HNLF when the two pumps were co-polarized (red dashed line) or orthogonally polarized (black solid line), is shown in the inset of Fig. 8 for the same total power of 20 dBm when no signal was present. The FWM components generated solely by the pump interactions were reduced by 30 dB for the cross-polarized case as compared to the co-polarized one, highlighting the difference in bandwidth occupation between the scalar and the polarization assisted PSA schemes. The comb tone used as the signal was modulated with a 2^{31}-1 pseudo-random bit sequence to generate a single-polarization 10 or 20 Gbaud BPSK or QPSK signal depending on the application to be demonstrated (phase regeneration or electric field decomposition). In the case of phase regeneration, the signal was sent through a noise module to emulate the effects of phase noise. This comprised either a single tone sinusoidal wave at 1.1 GHz or an ASE source followed by a 32 GHz photo-detector (PD) and a 20 GHz RF amplifier which were used to drive a phase modulator through which the signal was passed. The (noisy) signal was then combined with the pumps with the desired polarization and this was typically guaranteed by detecting part of the output signal after the HNLF and the filter (not shown in Fig. 8) using a slow photodetector and real time scope and minimizing the PSER in front of the polarizer. All the waves were amplified in a single EDFA up to a total power of either 20 dBm or 30 dBm (depending on the operation to be demonstrated) at the HNLF input. The 302 m long germanium-silicate dispersion shifted strained HNLF had a nonlinear coefficient of 11.6 $W^{-1}\cdot km^{-1}$, a dispersion slope of 0.018 $ps/(nm^2\cdot km)$, an average zero-dispersion wavelength (after straining) of 1555 nm, an SBS threshold of 27 dBm and a polarization mode dispersion (PMD) of 0.5 $ps/km^{0.5}$. Due to some small random birefringence of the HNLF, the pump orthogonality is not maintained along the fiber, creating a gain dependent on such small pump misalignments. However, in our experiments we tried to suppress these effects by optimizing the pump state of polarizations (SOPs) launched into the HNLF using a polarization controller (PC) at the input of the HNLF [25]. Examples of typical spectra at the output of the HNLF for the two power levels used are shown in Fig. 9. A small portion of the corresponding output (using the 1% output port of a tap coupler) was used to control the relative polarization of the various beams. The signal and the generated idler, which were at the same frequency, but on orthogonal polarizations, were filtered out and fed into a carefully aligned polarizer to achieve PS operation. In more detail, polarization alignment was performed by optimizing the signal performance, as monitored in the constellation analyzer. A PSER of 26.6 dB was obtained through spectral measurements at the output of the PSA which we believe was

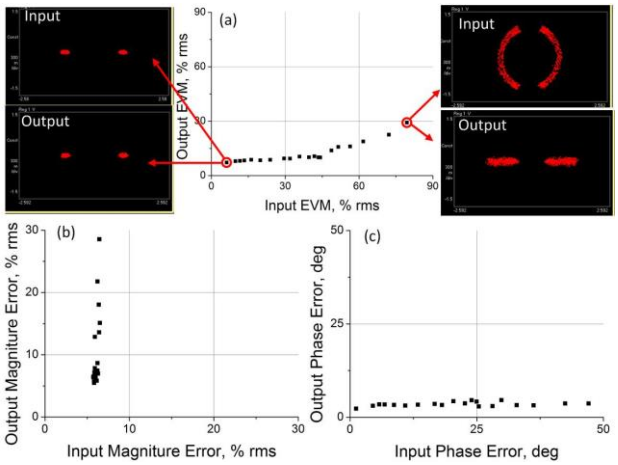

Fig. 10: Output versus input error vector magnitude (a), magnitude error (b) and phase error (c) taken from the constellation diagrams at different power level of sine wave into the phase modulator. Inset figure: constellation diagrams at (a) the input and (b) the output of the PA-PSA for a total input power of 20 dBm for no noise and two different levels of noise added to the signal.

mainly limited by the polarization extinction of the polarization maintaining components and the non-zero PMD of the HNLF used. PSERs of about 2.5 dB and 5.6 dB were measured when our set-up was modified to operate as either a vector PSA or a scalar PSA respectively, and while maintaining the same total power of 20 dBm (all schemes were based on dual-pump degenerate FWM). A detailed description of how the experimental set-up was modified and the comparison in terms of PSERs as a function of total input power among the various implemented PSA schemes was discussed and reported in [20]. The signal was then assessed using homodyne coherent detection followed by real time data analysis (optical modulation analyser, OMA). The local oscillator used in the measurement was obtained by tapping the signal laser before the amplitude modulator. The slow thermo-acoustic relative phase drifts were suppressed by monitoring the signal power at the PSA output and controlling the piezo-electric transducer (PZT) based fiber stretcher located in the path of the two pumps.

IV. Phase Regeneration of BPSK Signals

The PA-PSA operated at total input power of about 20 dBm (and giving rise to a NPS of about 0.35 rad) was initially assessed as a BPSK phase regenerator for a 20 Gbaud BPSK signal and the performance of the scheme was assessed for various types and levels of phase noise. In this instance, the signal to pump ratio was about -14 dB. Initially, the phase modulator used to degrade the signal phase was driven by a single sine wave at different power levels. The corresponding results at the input and output of the PA-PSA are summarized in Fig. 10 in terms of error vector magnitude (EVM), magnitude error (ME) and phase error (PE). When no noise was added to the signal, the performances at the input and output of the system were very comparable with EVMs of about 6-7 % rms, MEs of about 6 % rms and PEs of about 1-2 deg rms for both cases. As the input phase noise increased (up to 47 deg rms), the output phase noise remained fairly

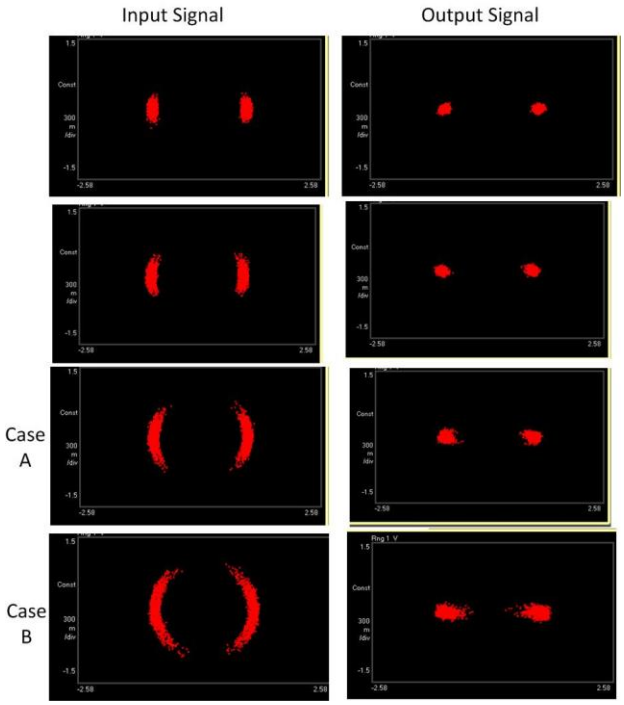

Fig.11: Measured constellation diagrams at the input and output of the polarization assisted PSA for different amount of broadband phase noise added.

constant (only slightly increasing to 3.7 deg rms), achieving an overall phase noise reduction of almost 13 times. Such impressive phase squeezing capabilities obviously came at the expense of the typical phase-to-amplitude conversion via a cosine amplitude transfer function (as shown in Fig. 2), since the system operated far from the saturation regime. For the highest level of phase noise added to the signal, an input ME of 6.5 % rms was degraded to 29 % rms, degrading the input signal amplitude by more than 4 times. However, the EVM values (which take into account both MEs and PEs) for all the various cases of phase noise added shows an overall improvement after the regenerator of almost 3 times (from 79.5 % rms to 29 % rms, respectively). Some examples of constellation diagrams at the input and output of the PSAs (when no noise or the highest level of noise was added to the signal) are also shown as insets in Fig. 10 for reference.

The system was then assessed using broadband phase noise, obtaining similar conclusions as in the single-tone case. Figure 11 shows the measured constellation diagrams for the BPSK signal at the input and output of the polarization assisted PSA for different amounts of emulated broadband phase noise. For example, considering the two higher values of added phase noise (labelled as Case A and Case B in Fig. 11), PEs of 14.4 deg rms (Case A) and 21.3 deg rms (Case B) could be squeezed down to 3.7 deg rms at the PSA output, achieving an overall phase noise reduction of almost 4 and 6 times, respectively. On the other hand, as discussed above, the input magnitude error was degraded from 5-6 % rms at the input to 8 % rms (Case A) and 12 % rms (Case B) at the output. However, the EVMs were improved from 26 % rms (Case A) and 37 % rms (Case B) at the input to 10 % rms and

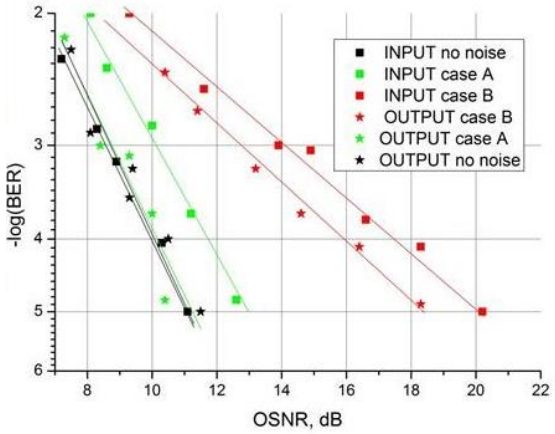

Fig.12: Measured BER curves at the input and output of the polarization assisted PSA for different amount of phase noise added.

13.5 % rms, respectively at the PA-PSA output, showing a significant overall performance improvement of almost 3 times in both cases.

The system was also characterized in terms of BER curves at the input (squares) and output (stars) of the PA- PSA, when no noise or the two higher levels of broadband phase noise were added to the signal, as shown in Fig. 12. When no noise was added to the signal, the PSA did not add any OSNR penalty as compared to the back-to-back operation (black symbols and lines). When phase noise corresponding to Case A was added to the signal, an OSNR penalty of almost 2 dB was measured at a BER of 10^{-5} (green squares). However, after the PSA, a similar performance to the back-to-back was observed (green stars). When severe phase noise was added to the signal (Case B, red squares) with a power penalty of about 9 dB as compared to the back-to-back operation, the PSA could still improve the system performance by about 2 dB as compared to its input (red stars), but it was not possible to obtain the same performance as in the back-to-back case due to the phase-to-amplitude conversion discussed above.

V. Simultaneous Electric Field Decomposition of Advanced Modulation Formats

While operating at the same power levels as before, the PA-PSA was then configured to simultaneously demodulate the in-phase and quadrature components of the signals. As discussed in Section II, two identical and π-phase shifted PSAs can be achieved by rotating the polarizer's transmission angles to α and $\pi-\alpha$, thus enabling quadrature component decomposition. For ease of implementation, in our experiment we chose to use a single polarizer and aligned the signal sequentially to the two PSAs. The results obtained for a 20 Gbaud QPSK signal are shown in Fig.13. The incoming QPSK signal has an EVM of about 7.5 % rms, ME of about 4.5 % rms and PE of about 3.5 deg rms, while the EVM, ME and PE were about 10 % rms, 7.5 % rms and 4 deg rms at the output for both of the I and Q components.

Similar measurements were then repeated when operating the PA-PSA at a higher total input power of 30 dBm (with a signal-to-pump ratio maintained at around -7 dB) using a 10

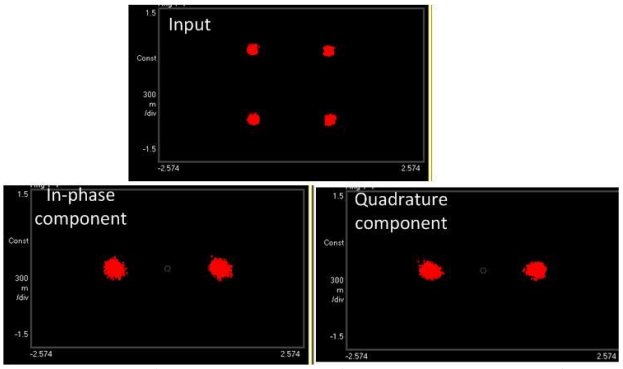

Fig.13: Electric field decomposition of a QPSK signal at NPS of about 0.35 rad.

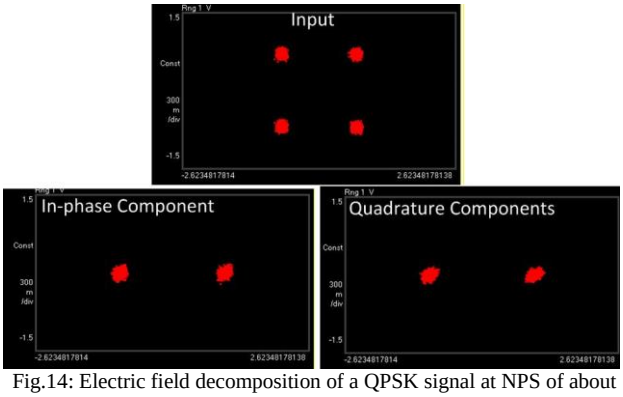

Fig.14: Electric field decomposition of a QPSK signal at NPS of about 3.5 rad.

Gbaud QPSK signal, obtaining very similar results. In this case, α was about $\pi/4$ rad, allowing a single PBS to be used, as discussed in Section II. The corresponding constellation diagrams are shown in Fig. 14. The EVM, ME and PE of the incoming QPSK signal were about 7.4 % rms, 5.2 % rms and 3.0 deg rms, respectively (Fig.13 (a)), while the corresponding values for both of the I and Q components ranged between 8.1- 8.5 % rms, 6- 6.7 % rms, and 3.1- 3 deg rms, respectively. The slight improvement in performance for higher versus lower NPSs, see Fig. 13 and Fig. 14, is mainly due to the PA-PSA losses that are reduced as the polarizer's angle approaches $\pi/4$.

A point to note in the implementation of this system is that the output (decomposed) signal cannot be used as the feedback for the phase synchronisation of the waves at the PSA input. This is because the power of QPSK signals at the output of degenerate dual-pump PSAs does not vary as a function of the phase and cannot be used to stabilize the incoming signal. However, by slightly modifying the configuration of the feedback control and introducing a phase comparator as proposed and demonstrated in [30], it is possible to use the 2nd -order FWM component of the QPSK signal as the feedback signal in a new degenerate dual-pump PSA and to accurately control and stabilize the gain axes of our PA-PSA. However, any small skewing of the original QPSK signal is reflected in small power variations of the demodulated signal as a function of the phase. While this did not give us enough stability to perform BER measurements, it

was sufficient for the purpose of the measurements reported in Fig. 13 and Fig.14.

VI. QPSK Phase Regeneration

The PA-PSA scheme working at high input total powers (around 30 dBm) and at saturation (signal-to-pump ratio around -2 dB) was then configured to perform phase regeneration of a 10 Gbaud QPSK signal. A single polarizer aligned to the original signal, i.e. at $\pm\pi/4$ with respect to either of the PSA gain axes in Fig. 4 was used, as discussed in Section II, to achieve both regeneration and recombination within the same fiber path.

The system was first tested without any phase noise added to the signal, see Fig. 15 (a) - (b), showing a small degradation at the system output. The EVM values were 8 % rms and 9 % rms at the input and output of the system, respectively. The QPSK signal was then degraded using a single-tone phase noise, see Fig. 15 (c) (following Section IV, it is anticipated that similar results would be obtained when using broadband phase noise). An EVM, ME and PE of ~20 % rms, 6 % rms and 11 deg rms, were measured, respectively. The PA-PSA regenerator was able to improve the signal performance, leading to EVM, ME and PE of 14 % rms, 8 % rms, and 6 deg rms, respectively, (Fig. 15 (d)) i.e. it reduced the initial phase noise by almost a half.

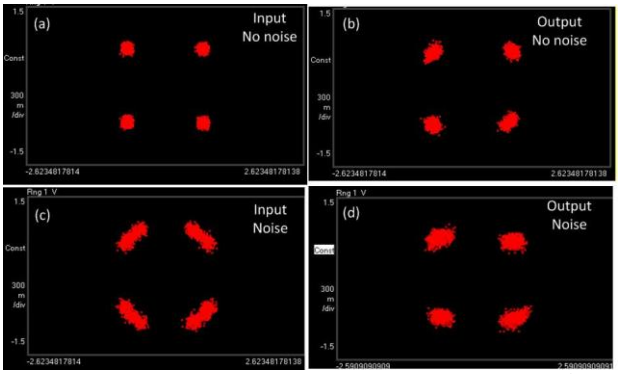

Fig.15: Measured constellation diagrams at the input and output of the scheme when it is implemented as a regenerator with and without noise.

VII. Conclusions

We have proposed and experimentally demonstrated a new optical processor for coherent optical signals by simultaneously extracting the two (in-phase and quadrature) quadrature components at the same frequency, by using two identical and π-phase shifted PSAs in a single HNLF. This new phase sensitive signal processor, the polarization assisted PSA, is based on a degenerate dual-pump vector parametric amplifier followed by mixing the polarization of the phase-locked signal/idler pair. The PA-PSA was demonstrated to exhibit a binary step-like phase response and allow PSERs as high as 26.6 dB at nonlinear phase shifts as low as 0.35 rad.

A few possible examples highlighting the potential of the scheme were experimentally demonstrated: (i) phase regeneration/ squeezing of BPSK signals, showing ~2dB OSNR improvement compared to an input signal affected by broadband phase noise, (ii) simultaneous decomposition of the two quadratures of QPSK signals and (iii) phase regeneration of a QPSK signal achieving a phase noise reduction of almost one half.

IV. Acknowledgments

We would like to thank OFS for supplying the HNLF used in this experiment.

References

[1] K. K. Y. Wong et al., "Polarization-Independent Two-Pump Fiber Optical Parametric Amplifier", IEEE Photonic Technology Letters, vol. 14, p. 911-912, 2002

[2] B. P.-P. Kuo et al., "Transmission of 640-Gb/s RZ-OOK Channel Over 100-km SSMF by Wavelength-Transparent Conjugation", Journal of Lightwave Technology, vol. 29, p. 516-523, 2011

[3] P. Devgan et al., "Highly efficient multichannel wavelength conversion of DPSK signals", Journal of Lightwave Technology, vol. 24, p. 3677-3682, 2006

[4] A. H. Gnauck et al.,"All-Optical Tunable Wavelength Shifting of a 128-Gbit/s 64-QAM Signal", ECOC Th2.F.2, 2012

[5] X. Li et al., "Wavelength conversion of 544-Gbit/s dual-carrier PDM-16QAM signal based on the co-polarized dual-pump scheme", Optics Express, vol. 20, p.21324-21330, 2012

[6] J. Yu et al., "In-band Wavelength Conversion of 16x114-Gbps Polarization Multiplexed RZ-8PSK Signals with Digital Coherent Detection", OFC OThS7, 2009.

[7] V. J. F. Rancaño, et al., "100-GHz grid-aligned multi-channel polarization insensitive black-box wavelength converter", Journal of Lightwave Technology Vol. 32 (17) pp. 3027 - 3035, (2014).

[8] K. Croussore, G. F. Li, " Phase regeneration of NRZ-DPSK signals based on symmetric-pump phase-sensitive amplification", IEEE Photon. Technol. Lett. 19, 864–866 (2007).

[9] R.Slavík et al.,"All-optical phase and amplitude regenerator for next-generation telecommunications systems," Nature Photonics, vol. 4, no. 10, pp. 690–695, Oct. 2010.

[10] J. Kakande et al., "Multilevel quantization of optical phase in a novel coherent parametric mixer architecture", Nature Photonics, vol. 5, no. 12, pp. 748–752, Dec. 2011.

[11] M. Gao, T. Kurosu, T. Inoue and S. Namiki, "Efficient phase regeneration of DPSK signal by sideband-assisted dual-pump phase sensitive amplifier", Electronics Lett., 39 (2), 140-141 (2013).

[12] Z. Tong, et al., "Towards ultrasensitive optical links enabled by low-noise phase-sensitive amplifiers", Nature Photonics, vol. 5, pp. 430-436, 2011.

[13] T. Umeki, et al., "First demonstration of high-order QAM signal amplification in PPLN-based phase sensitive amplifier", Optics Express, vol. 22 (3), pp. 2473-2482, 2014.

[14] M. Gao et al., "Low-penalty Phase De-multiplexing of QPSK Signal by Dual-pump Phase Sensitive Amplifiers", ECOC, We.3.A.5 (2013).

[15] R. P. Webb, et al., "Phase-sensitive frequency conversion of quadrature modulated signals," Opt. Express 21, 12713–12727 (2013).

[16] F. Da Ros, et al., "QPSK-to-2×BPSK wavelength and modulation format conversion through phase-sensitive four-wave mixing in a highly nonlinear optical fiber", Optics Express 21 (23), pp. 28743-28750 (2013).

[17] J. Kakande, F. Parmigiani, R. Slavík, D. J. Richardson, "Homodyne operation of a phase-only optical amplifier", European Conference on Optical Communication (ECOC) Amsterdam, Th.1.F.3, (2012).

[18] C. J. McKinstrie and S. Radic, "Phase-sensitive amplification in a fiber", Opt. Exp. 12, 4973-4979 (2004).

[19] M. Vasilyev, "Distributed phase-sensitive amplification", Optics Express, 13 (19), 7563-7571 (2005).

[20] F. Parmigiani, et al., "Optical Phase Quantizer Based on Phase Sensitive Four Wave Mixing at Low Nonlinear Phase Shifts", IEEE Photonics Technology Letters, 26 (21), pp.2146-2149, (2014).

[21] A. L. Riesgo, et al., "Demonstration of Degenerate Vector Phase-Sensitive Amplification", We.3.A.3, ECOC 2013.

[22] Takayuki Kurosu, et al., "Phase regeneration of phase encoded signals by hybrid optical phase squeezer", Optics Express, Vol. 22, Issue 10, pp. 12177-12188 (2014).

[23] F. Parmigiani, et al., “Efficient binary phase quantizer based on phase sensitive four wave mixing”, European Conference on Optical Communication (ECOC) Cannes, Tu.1.4.1, (2014).
[24] F. Parmigiani, et al., “Quadrature decomposition of optical fields using two orthogonal phase sensitive amplifiers”, European Conference on Optical Communication (ECOC) Cannes, Tu.4.6.2, (2014).
[25] A. Lorences-Riesgo, et al., “Experimental analysis of degenerate vector phase-sensitive amplification” Opt. Express, vol. 22, no. 18, pp. 21889-21902 (2014).
[26] E. R. Martins, D. H. Spadoti, M. A. Romero, and B.-H. V. Borges, “Theoretical analysis of supercontinuum generation in a highly birefringent D-shaped microstructured optical fiber”, Opt. Express 15 (22), 14335-14347 (2007).
[27] F. Poletti and P. Horak, “Description of ultrashort pulse propagation in multimode optical fibers”, J. Opt. Soc. Am. B 25 (10), 1645-1654 (2008).
[28] Q. Lin and G. P. Agrawal, “Vector theory of four-wave mixing: polarization effects in fiber-optic parametric amplifiers,” J. Opt. Soc. Am. B, Vol. 21, Issue 6, pp. 1216-1224 (2004).
[29] Z. Zheng, et al., "All-optical regeneration of DQPSK/QPSK signals based on phase-sensitive amplification," Optics Communications, vol. 281, pp. 2755-2759, 2008.
[30] M. Gao, T. Kurosu, T. Inoue, S. Namiki, “Phase Comparator using Phase Sensitive Amplifier for Phase Noise-Tolerant Carrier Phase Recovery of QPSK Signals”, TuS2-4, OECC/PS (2013).

Francesca Parmigiani was born in Milan, Italy. She graduated with honours in Electronic Engineering at Politecnico di Milano, Milano, Italy, in 2002, and received the Ph.D. degree in optical communication systems at the Optoelectronics Research Centre (ORC), University of Southampton, U.K in 2006. She is currently a Senior Research Fellow at the ORC. In April 2010 she was awarded a prestigious Postdoctoral Research Fellowships from the Royal Academy of Engineering, in support of her research on the combination of all-optical signal processing and advanced modulation formats. Her research has produced more than 155 papers in journals and conferences in the field of optical communications. Her research interests include ultra-fast all-optical sampling techniques, pulse shaping using specialized fiber Bragg gratings, all-optical nonlinear processing and switching mainly in optical fibers, as well as advanced modulation formats.
Dr Parmigiani is a member of the Optical Society of America (OSA).

Dr Graham Hesketh graduated with first class hons. in Physics with Astrophysics from the University of Canterbury, UK in 2009. He received the MSc degree in Quantum Fields and Fundamental Forces from Imperial College London, UK in 2010 and the PhD degree in Nonlinear Effects in Multimode Optical Fibres from the Optoelectronics Research Centre (ORC), University of Southampton, UK in 2014.
Dr. Hesketh is a resarch fellow at the ORC. His research interests lie in the fields of optical communications, all-optical signal processing and nonlinear fibre technology.

Radan Slavík (M’07–SM’07) received the M.A.Sc. and Ph.D. degrees in optics and optoelectronics from the Faculty of Mathematics and Physics, Charles University in Prague, in 1996 and 2000, respectively. He received D.Sc. degree from Academy of Sciences of the Czech Republic in 2009.

In 1995-2000 and 2004-2009 he was with the Institute of Photonics and Electronics, Czech Academy of Sciences in Prague. In 2000-2003, he was with the Centre d’optique, photonique et laser at Université Laval, Québec, Canada as a Postdoctoral Research Fellow. From 2009 he is with Optoelectronics Research Centre (ORC), University of Southampton, Southampton, U.K. His research interests focus in optical and optics-assisted signal processing.

R. Slavík is a member of OSA. In 2006, he received Otto Wichterle Award and in 2007, he received The Visegrad Group Academies Young Researcher Award.

Peter Horak received his MSc and PhD degrees in theoretical physics from the University of Innsbruck, Austria, in 1993 and 1997, respectively. Since 2001 he has been with the Optoelectronics Research Centre, University of Southampton, UK, where he now an Associate Professor. He is interested in the theoretical and numerical investigation of photonic devices and systems, including linear, nonlinear and quantum optical effects.

Prof Periklis Petropoulos graduated from the Department of Electrical Engineering and Information Technology, University of Patras, Greece in 1995. He received the MSc degree in Communications Engineering from the University of Manchester Institute of Science and Technology, UK in 1996 and the PhD degree in Optical Telecommunications from the Optoelectronics Research Centre (ORC), University of Southampton, UK in 2000. Dr. Petropoulos is a Professor of Optical Communications at the ORC. His research interests lie in the fields of optical communications, all-optical signal processing and nonlinear fibre technology. He has participated in several European Union and national research projects in the field of optical communications. His research has produced more than 350 papers in technical journals and conference proceedings, including several invited and post-deadline papers in major international conferences, and holds 6 patents. Dr. Petropoulos is a Senior Member of the Optical Society of America. He has served as member of the Technical Programme Committees for several international conferences, including the European Conference on Optical Communication (ECOC), the Optical Fiber Communication (OFC) conference and the European Conference on Lasers and Electro-Optics (CLEO/Europe). He is the Chair of the “Photonic Subsystems for Digital System Applications” Subcommittee of OFC’2015.

Prof David J. Richardson FIEEE, joined the Optoelectronics Research Centre (ORC) at the University of Southampton UK as a Research Fellow in 1989. He was awarded a Royal Society University Fellowship in 1991 in recognition of his pioneering work on short pulsed fiber lasers. He is now a Deputy Director of the ORC and responsible for much of the ORC's fiber related activities. His current research interests include amongst others: optical fiber communications, microstructured optical fibers and high power fiber lasers. He has published more than 1000 conference and journal papers during his time at the ORC and produced more than 20 patents. He was one of the cofounders of SPI Lasers Ltd., an ORC spin-off venture acquired by the Trumpf Group in 2008. Prof. Richardson is a Fellow of the Optical Society of America, the Institute of Engineering and Technology and the Royal Academy of Engineering and is currently the holder of a Royal Society Wolfson Research Merit Award.